AWARD NUMBER: W81XWH-20-1-0063

TITLE: Identifying Antigen-Specific T and B Cells in Seronegative Rheumatoid Arthritis Synovial Tissue: Implications for Antigen-Specific Immunotherapy

PRINCIPAL INVESTIGATOR: Professor Ranjeny Thomas

CONTRACTING ORGANIZATION: The University of Queensland, Brisbane, Australia

REPORT DATE: March 2021

TYPE OF REPORT: Annual report

PREPARED FOR: U.S. Army Medical Research and Development Command
Fort Detrick, Maryland 21702-5012

REPORT DOCUMENTATION PAGE	Form Approved OMB No. 0704-0188

1. REPORT DATE	**2. REPORT TYPE**	**3. DATES COVERED**
March 2021	Annual	15Feb2020-14Feb2021

4. TITLE AND SUBTITLE
Identifying Antigen-Specific T and B Cells in Seronegative Rheumatoid Arthritis Synovial Tissue: Implications for Antigen-Specific Immunotherapy.

5a. CONTRACT NUMBER

5b. GRANT NUMBER
W81XWH-20-1-0063

5c. PROGRAM ELEMENT NUMBER

6. AUTHOR(S)
Ranjeny Thomas, Mihir Wechalekar, Helen McGuire, Pascale Wehr

E-Mail:Ranjeny.thomas@uq.edu.au

5d. PROJECT NUMBER

5e. TASK NUMBER

5f. WORK UNIT NUMBER

7. PERFORMING ORGANIZATION NAME(S) AND ADDRESS(ES)

The University of Queensland
St Lucia, Brisbane
QLD 4072, Australia

8. PERFORMING ORGANIZATION REPORT NUMBER

9. SPONSORING / MONITORING AGENCY NAME(S) AND ADDRESS(ES)

U.S. Army Medical Research and Development Command
Fort Detrick, Maryland 21702-5012

10. SPONSOR/MONITOR'S ACRONYM(S)

11. SPONSOR/MONITOR'S REPORT NUMBER(S)

12. DISTRIBUTION / AVAILABILITY STATEMENT

Approved for Public Release; Distribution Unlimited

13. SUPPLEMENTARY NOTES

14. ABSTRACT
We characterized clonally-expanded T cells in blood and synovial tissue (ST) of 4 seropositive rheumatoid arthritis (RA) patients. Using simultaneous single-cell RNA and T cell receptor (TCR)α/β sequencing, we identified T cell clonotypes in paired blood and ST of newly-diagnosed, seropositive, treatment-naïve HLA-DRB1*04:01+ RA patients. The transcriptomic signatures of ST-unique CD4+ TCR clonotypes highlight central memory, Th2 differentiation and IL-6 signaling. Unexpectedly, the most expanded circulating CD4+ and CD8+ clonotypes display cytotoxic polyfunctional proinflammatory capacity. Among these, TCR sequencing and tetramer staining identified EBV- and CMV-specific clonotypes, some of which migrated to ST, lodging adjacent to blood vessels and dendritic cells. Our findings implicate antigen-specific Th2 and central memory CD4 T cells and cytotoxic viral-specific bystander T cell clones in early RA synovial inflammation.

15. SUBJECT TERMS
rheumatoid arthritis, seropositive, seronegative, synovial tissue, T cells, B cells, dendritic cells, oligoclonal expansion

16. SECURITY CLASSIFICATION OF:			17. LIMITATION OF ABSTRACT	18. NUMBER OF PAGES	**19a. NAME OF RESPONSIBLE PERSON**
a. REPORT	b. ABSTRACT	**c. THIS PAGE**			USAMRMC
Unclassified	**Unclassified**	Unclassified	Unclassified	17	**19b. TELEPHONE NUMBER** *(include area code)*

Table of Contents

1. Introduction 1
2. Keywords 1
3. Accomplishments 1
4. Impact 4
5. Changes/Problems 4
6. Products 4
7. Participants & Other Collaborating Organizations 5
8. Special Reporting Requirements 6
9. Appendices 7

1. Introduction

There is considerable unmet need for better early molecular biomarkers to stratify treatments directed towards the pathogenesis of seronegative RA. In the last few years, joint synovial biopsies have considerably advanced the understanding of RA pathogenesis. In particular, it has become clear that different synovial pathological features, including lymphocyte-rich and lymphocyte-poor (myeloid cell and fibroblast rich) subtypes (also called "pathotypes") distinguish patient subgroups [1]. During the RA autoimmune response, autoantigen-specific naïve or memory B cells form antibody-producing plasmablasts, which transiently circulate in the blood before forming memory B cells or synovial tissue-resident plasma cells. Seropositive RA patient synovial tissue has been described to be infiltrated by lymphoid aggregates, including oligoclonal T cells and citrullinated antigen-specific plasmablasts in ectopic lymphoid tissue structures (ELS) [2]. However, much less is known about seronegative RA synovial tissue, as it has not been comprehensively studied. In this project, we hypothesize that synovial tissue of a large fraction of seronegative RA patients is infiltrated by antigen-specific T cells responding to local antigen presentation by B cells, fibroblasts, and/or dendritic cells (DC). The objective of this proposal is to further the mechanistic understanding of antigen-specific responses in seronegative RA by characterising synovial antigen-presenting B cell and T cell clonotypes and their relationship in ACPA-negative RA patient biopsies to inflammatory fibroblasts, DC and other innate cells, and to compare this with ACPA+ patient biopsies.

2. Keywords

rheumatoid arthritis, seropositive, seronegative, synovial tissue, T cells, B cells, dendritic cells, oligoclonal expansion

3. Accomplishments

Major Task 1 (year 1)	Months			
1. Obtain HRPO/ACURO approvals	1-3	PI Thomas		
2. Hire post-doc and technician	1-3		PI Wechalekar	
3. Order sequencing kits	1-3	PI Thomas		
4. Ship seropositive RA and control samples from site 2 to site 1 and plan experiment details with Genomics Facility	4	PI Thomas		
5. Sequence seropositive RA and control samples	4-5	PI Thomas		
6. Bioinformatic analysis of scRNAseq and TCRseq data: seropositive RA relative to controls	6-12	PI Thomas		
7. Bioinformatic analysis of BCR seq data: V_H and V_L immunoglobulin gene sequences	6-12			PI Robinson
8. Arthroscopic biopsy of seronegative RA patients, store tissues	3-12		PI Wechalekar	
9. Express recombinant antibodies representative of affinity-matured clonal families	9-15			PI Robinson
10. Design and build imaging mass cytometry panel using inflammatory OA and tonsil sections	4-6	PI Thomas		
11. Imaging mass cytometry on frozen tissue sections of seropositive RA	8-12	PI Thomas		
Milestones Achieved	*Month*			
HRPO/ACURO Approval	3	24 Sept 20		
Seropositive RA samples shipped and sequenced	5	*20 Dec 20*		
Completed bioinformatic analysis of seropositive RA data	12	*50% complete*		

Obtained 12 seronegative RA synovial biopsies at arthroscopy and clinically characterized, HLA typed	12	*25% complete*		
Expressed and characterized recombinant antibodies	15	*0% complete*		
Completed imaging mass cytometry seropositive RA tissues	12	*50% complete*		

Specific Aims

Aim (major task) 1: To identify oligoclonally expanded T cell and clonal plasmablasts and memory B cells in synovial tissue of clinically well-characterized, HLA-typed new-onset untreated ACPA+ RA.

Aim (major task) 2: To identify oligoclonally expanded T cell and clonal plasmablasts and memory B cells in synovial tissue of clinically well-characterized, HLA-typed new-onset untreated ACPA-RF- RA.

Significant results

Preamble: While waiting for the HRPO approval for this project, we began by single cell RNA/T cell receptor (but not B cell receptor) sequencing paired peripheral blood mononuclear cells (PBMC) and disaggregated cells from stored synovial tissue biopsies that had been collected from 4 patients with seropositive RA. With the availability of this sequencing data, we were able to establish our bioinformatics pipeline for the entire project. As the sequencing was analyzed, we established the imaging mass cytometry panel, techniques and analysis pipeline. The results of these studies are reported in a manuscript (submitted for publication) entitled: Antigen-expanded T cells infiltrating new-onset rheumatoid arthritis synovium are IL-6-reponsive, Th2 and inflammatory viral-specific clones.

Summary of the major findings:

RA is one of the best-described autoimmune diseases, based on an appreciation of the susceptibility HLA class II risk alleles and autoimmunity to citrullinated self-peptides, where ACPA is a very specific diagnostic test. Joint inflammation is driven by T cells responding to antigen presentation by dendritic cells and B cells, resulting in macrophage and fibroblast-driven synovial tissue cytokine production. All current treatment strategies suppress inflammation by interfering with the interactions or inflammatory products of these cell types. However, none is curative, highlighting deficiencies in our understanding of the underlying autoimmune mechanisms of RA. A key unanswered question is how T cells, expanded by antigen, contribute to the onset of synovial inflammation. While technologies such as single cell RNA sequencing applied to the synovial (tissue and fluid) compartment have expanded knowledge of the infiltrating T cell populations, current understanding of their role in disease is largely based on studies of late-stage disease after treatment with disease modifying drugs, which may not accurately represent the disease onset.

We characterized clonally-expanded T cells in paired blood and synovial tissue of recently-diagnosed ACPA+, treatment-naïve HLA-DRB1*04:01+ RA patients with simultaneous single-cell RNA and T cell receptor α/β sequencing, tetramer staining and mass cytometry imaging.

We found that synovial-unique CD4+ TCR clonotypes displayed signatures of central memory, Th2 differentiation and IL-6 signaling, consistent with their local tissue interactions with antigen presenting cells. Unexpectedly, synovial tissue T cells with polyfunctional proinflammatory capacity derived specifically from clonally-expanded cytotoxic CD4 and CD8 T cells, including EBV and CMV-specific clonotypes (see detailed results in appendix).

Conclusions:

T cell clones exclusive to the ST were CD4+, oligoclonally expanded, and expressed signatures of central memory tissue-resident, Th2-like, and IL-6 responsive functional profiles. ICOS, which was expressed by ST memory T cells is important for their expansion and differentiation to follicular and peripheral helper T cells (Tfh/Tph). However, unlike ST from late-stage RA, we found no signature of Tfh or Tph in these early-stage STs. Transcriptomic evidence of IL-6 signaling provides clues to their environmental interactions. Using immunohistochemistry and imaging mass cytometry, we found that ST IL-6 staining was located peri-vascularly and IL6 transcripts projected mainly to CD90+ fibroblasts and CD14+ APCs – also located per-vascularly. Together our data suggest that these clones are signaled by IL-6-producing APCs encountered in ST.

Of interest, despite infiltration by clonally-expanded CD4+ memory T cells – including B cell helper phenotypes – the ST biopsies of these very early ACPA+ RA patients generally lacked significant B cell infiltration, or ectopic lymphoid tissue organization. It is likely that the memory T cells infiltrating ST were previously primed in lymph nodes, such as those draining mucosal sites [3,4] and that ACPA+ plasmablasts are located – at least in these cases – in lymph nodes, spleen and bone marrow. It will be of interest to determine whether the lack of ST B cells holds true for the remaining seropositive samples to be studied in this project. Furthermore, it will be of great interest to link the transcriptome of the oligoclonally expanded T cells in seronegative RA ST, the signaling signatures they manifest and their relationship to B cells and other antigen-presenting cells.

Our finding that T cell-driven inflammation derives from cytotoxic T cells (of which 2-42% in ST were viral-specific) in patients not yet treated with potentially immunosuppressive drugs strongly implicates viral-specific bystander T cells in the development of synovial inflammation. Their functional profile suggests these synovial bystander cells contribute to IFN-γ- and TNF-mediated inflammation and CTL-mediated tissue destruction. An EBV-driven immunopathological mechanism has been proposed in multiple sclerosis, where CNS-infiltrating EBV-specific CD8+ CTL amplify inflammation [5], and similar mechanisms appear to be likely in RA. Bystander activation has been exemplified in an experimental mouse model of RA, where antigen-specific T cells recruited to the inflammatory site were vastly outnumbered by non-antigen-specific activated CD4+ and CD8+ T cells [6]. It will also be of interest to model whether immunotherapy directed against the inciting antigen or viral specific antigens improves arthritis.

Key technical achievements for this reporting period
Established bioinformatics pipeline for single cell RNA/TCR sequencing pipeline
Established mass cytometry imaging in frozen sections of RA synovial tissue

Opportunities for training and professional development
PhD student Pascale Wehr worked on this project. She was mentored by a senior graduate student, Chenhao Zhao and Ahmed Mehdi to develop bioinformatics skills to complete the analysis. Three PIs on this project: Ranjeny Thomas, Helen McGuire and Mihir Wechalekar and their teams provided advice and support on imaging mass cytometry, clinical aspects and background context on RA pathogenesis. The PI multi-disciplinary team met monthly as a whole, which stimulated professional development of all team members across the range of disciplines represented in this project. The work was presented at institutional seminars which provided valuable feedback and advice from the audience to the team members.

Dissemination
The preliminary results have been presented in talks and seminars to rheumatologists and scientists.
Next reporting period goals
1. Complete the analysis of seropositive RA samples
We have now sequenced an additional 7 seropositive paired samples, including BCR sequencing. BCR data will be transferred to Prof Robinson in Q2 2021. Analysis will proceed during 2021
2. Complete recruitment and analysis of seronegative RA samples
Recruitment is underway, initial imaging mass cytometry will proceed from Q2 2021 and sequencing and analysis will proceed once recruitment/biopsy is complete (towards end of 2021).

References

1. Orr, C. et al. Synovial tissue research: a state-of-the-art review. *Nat Rev Rheumatol* **13**, 463-475 (2017).
2. Corsiero, E. et al. Single cell cloning and recombinant monoclonal antibodies generation from RA synovial B cells reveal frequent targeting of citrullinated histones of NETs. *Ann Rheum Dis* **75**, 1866-75 (2016).
3. Demoruelle, M.K., Wilson, T.M. & Deane, K.D. Lung inflammation in the pathogenesis of rheumatoid arthritis. *Immunol Rev* **294**, 124-132 (2020).
4. O'Neil, L.J. & Kaplan, M.J. Neutrophils in Rheumatoid Arthritis: Breaking Immune Tolerance and Fueling Disease. *Trends Mol Med* **25**, 215-227 (2019).

5. Serafini, B., Rosicarelli, B., Veroni, C., Mazzola, G.A. & Aloisi, F. Epstein-Barr Virus-Specific CD8 T Cells Selectively Infiltrate the Brain in Multiple Sclerosis and Interact Locally with Virus-Infected Cells: Clue for a Virus-Driven Immunopathological Mechanism. *Journal of Virology* **93**, e00980-19 (2019).
6. Prendergast, C.T. et al. Visualising the interaction of CD4 T cells and DCs in the evolution of inflammatory arthritis. *Annals of the Rheumatic Diseases* **77**, 579-588 (2018).
7. Imberti, L. et al. Reduced T-cell repertoire restrictions in abatacept-treated rheumatoid arthritis patients. *Journal of Translational Medicine* **13**, 12 (2015).
8. Scarsi, M., Ziglioli, T. & Airo, P. Decreased circulating CD28-negative T cells in patients with rheumatoid arthritis treated with abatacept are correlated with clinical response. *J Rheumatol* **37**, 911-6 (2010).
9. Scarsi, M., Ziglioli, T. & Airo, P. Baseline numbers of circulating CD28-negative T cells may predict clinical response to abatacept in patients with rheumatoid arthritis. *J Rheumatol* **38**, 2105-11 (2011).
10. Bergot, A.S. et al. Regulatory T Cells Induced by Single-Peptide Liposome Immunotherapy Suppress Islet-Specific T Cell Responses to Multiple Antigens and Protect from Autoimmune Diabetes. *J Immunol* **204**, 1787-1797 (2020).

4. Impact

Impact on the discipline of rheumatology

Knowledge impact

The observations from the project to date highlight the critical input of viral-specific bystander T cells to RA synovial inflammation. Our observations also suggest a hypothesis about why RA develops in people with genetic susceptibility HLA-DR alleles. Patients with HLA-DR shared epitope alleles may have reduced adaptive immune capacity to achieve anti-viral immune resilience, leading to a more diverse and expanded cytotoxic and proinflammatory T cell repertoire. This may put them at risk of greater bystander inflammatory consequences, particularly in the context of other pathogen and damage-associated adjuvants at mucosal interfaces such as the lung, periodontium and the gut.

Our data also have important implications for design of future immunotherapies to control both self-specific and viral-specific T cells before and after RA onset. Treatment of RA patients with abatacept and TNF inhibitors was found to decrease oligoclonally-expanded cytotoxic $CD8^{+}$ $CD28^{null}$ memory T cells, and the pre-treatment frequency of these cells identified patients likely to respond to abatacept [7-9]. We have also shown that antigen-specific immunotherapy controls bystander CD8+ cytotoxic T cells in mice [10]. Thus it is very important to understand whether antigen-specific immunotherapy controls bystander cytotoxic T cells in patients with RA, and single cell RNA/T cell receptor sequencing should be a powerful technology to elucidate this.

Impact on other disciplines

The techniques developed in this project can be immediately applied to other autoimmune diseases in order to compare outcomes.

Impact on technology transfer

Nothing to report

Impact on society

Nothing to report

5. Changes/Problems

Changes in approach

Due to the delay in HRPO approval we went ahead with analysis of sequencing data from 4 of the 12 paired samples from seropositive RA (minus B cell receptor (BCR) sequencing) and established the technical pipelines for the research.

Delays and plans to resolve them

The COVID-19 pandemic reduced the capacity for clinical sample collection from seronegative RA patients from March to September 2020. Since the resumption of clinical research Dr Wechalekar has collected blood and ST from 3 patients and the remainder will be collected in 2021.

There were no changes with significant impact on expenditure or care of human subjects.

6. Products

Submitted for publication

Antigen-expanded T cells infiltrating new-onset rheumatoid arthritis synovium are IL-6-reponsive, Th2 and inflammatory viral-specific clones

Pascale Wehr, Hendrik J Nel, Chenhao Zhou, Ahmed M Mehdi, Helen McGuire, Helen Weedon, Annabelle Small, Raymond Steptoe, Stephanie Gras, Mihir D Wechalekar, Ranjeny Thomas
Acknowledgement of federal support: yes

Websites

Once published the paper will be accessible from https://espace.library.uq.edu.au/

Technologies or techniques

Bioinformatics code, sequencing data and imaging mass cytometry technical information will be available in public repositories and from the authors

Inventions, patents

None

Other products

Bioinformatics code
Sequencing data
Biospecimens (biopsy material)

7. Participants & Other Collaborating Organizations

Name	Pascale Wehr
Project role	Graduate student
Researcher identifier	
Nearest person month worked	12
Contribution to the project	Ms Wehr developed the bioinformatics pipeline and analysed the samples, created figures, wrote initial draft of manuscript
Funding support	PhD scholarship
Name	Hendrik Nel
Project role	Postdoctoral fellow
Researcher identifier	0000-0003-4374-7246
Nearest person month worked	2
Contribution to the project	Dr Nel assisted Ms Wehr with the sample disaggregation, sorting, sequencing set up and planning, and planning and trouble-shooting imaging mass cytometry
Funding support	European Union grant
Name	Chenhao Zhou
Project role	Graduate student
Researcher identifier	0000-0001-7702-3436
Nearest person month worked	2
Contribution to the project	Mr Zhou assisted Ms Wehr on the development of the bioinformatics pipeline, shared code, helped with trouble shooting and data analysis
Funding support	PhD scholarship
Name	Ahmed Mehdi
Project role	Postdoctoral fellow in bioinformatics
Researcher identifier	0000-0002-9300-2341
Nearest person month worked	1
Contribution to the project	Dr Mehdi assisted Ms Wehr on the development of the bioinformatics pipeline, shared code, helped with trouble shooting and data analysis
Funding support	
Name	Annabelle Small
Project role	Postdoctoral fellow
Researcher identifier	0000-0001-6275-2847
Nearest person month worked	1
Contribution to the project	Dr Small developed the imaging mass cytometry, identified suitable samples and stained them.

Funding support	
Name	Helen McGuire
Project role	Co-PI
Researcher identifier	0000-0003-2047-6543
Nearest person month worked	3
Contribution to the project	Dr McGuire planned the imaging mass cytometry, led the analysis, managed the staining and shipping and analysed the tissues, created figures.
Funding support	Ramaciotti Foundation
Name	Mihir Wechalekar
Project role	Co-PI
Researcher identifier	0000-0001-6668-9638
Nearest person month worked	3
Contribution to the project	Dr Wechalekar identified suitable patients for biopsy, identified suitable samples for analysis, provided deidentified HLA typing and clinical data, organised shipping, analysed tissue staining data in light of sequencing analysis
Name	Ranjeny Thomas
Project role	PI
Researcher identifier	0000-0002-0518-8386
Nearest person month worked	3
Contribution to the project	Prof Thomas supervised Ms Wehr, coordinated and met with the team, reviewed the data and set next steps, co-wrote first draft of manuscript with Ms Wehr.
Funding support	University of Queensland

No change to personnel

No other organizations involved besides those of the PIs.

8. Special Reporting Requirements

9. Appendices

Definition of four T cell superclusters in PB and ST, with enrichment of Th2 and cytotoxic effector T cells in ST

To characterize the T cells, we sub-clustered cells expressing *CD3D* (C2, 6, 8), then filtered to retain cells with a productive, full-length TCRα and TCRβ sequence (hereafter referred to as $CD3^+TCR^+$ cells). We identified 9 T cell clusters, broadly representing 4 T cell superclusters; cytotoxic T cells (*GZMB*; $CD4^+$ T C6, $CD8^+$ T C1, C4), $CD4^+$ T regulatory (Treg) (*FOXP3*, *CTLA4*; C7), $CD4^+$ Th2-like (*CD44*, *GATA3*; C0, C5) and central-memory-like (*CD44*, *CCR7*, *SELL*; $CD4^+$ T C2, C3, $CD8^+$ T C8) T cells (**Fig. 1A**). Cells in C9 were tentatively assigned as pro-inflammatory CD4/CD8 double-positive (DP) (*S100A8*, *S100A9* and *NEAT1*) [11], and were absent in ST (**Fig. 1D**). C12 was assigned as cytotoxic NK cells (*FCGR3A*, *IFNG*, *PRF1*, *GZMB*).
The C0 Th2-like cluster also expressed *TNFRSF4* (OX40), *ITGB1* (integrin beta-1), *CD69* (tissue-resident memory signature), *AREG* (amphiregulin, which characterizes mouse Th2 [12]) in addition to the Th2-associated transcription factor *GATA3*. C5 expressed a similar transcriptomic profile to C0 but downregulated certain activation/differentiation markers, including *CD69*, suggesting that cells in C0 and C5 may reflect two effector/maturation states. Pseudotime trajectory analysis – providing a quantitative measure of cellular progression through differentiation [13] – supported this proposition, with C0 derived from C5 and further along the same trajectory path (**Fig. 1C**). Gene Set Enrichment Analysis (GSEA) confirmed enrichment of hallmark Th2 gene signatures rather than Th1 or Th17 signatures in C0 (**Fig. 1B**).
DGE analysis revealed that C3 resembled a more mature central-memory-like state of the same naïve-like $CD4^+$ cell type, C2 – a hypothesis supported by pseudotime trajectory analysis (**Fig. 1C**). Despite *ICOS* expression, C3 did not have features of T_{FH}/T_{PH} (**Fig. 1B** CD4 T_{FH}/T_{PH}, Zhang, et al. [14]). C7 was the only cluster to express *FOXP3*, and also expressed *CTLA4* and *TIGIT*. We thus classified C7 as an activated $CD4^+$ Treg cluster (**Fig. 1B**). C1 expressed high levels of granzymes (*GZMB*, *GZMA*, *GZMH*), *IFNG* and *TNF*. C4 expressed a similar profile, albeit less effector-like than C1 with less *GZMB* and *IFNG* but higher *GZMK* transcript expression). Consistent with a strong contribution to synovial inflammatory cytokine production, *IFNG* and *TNF* transcripts in ST predominantly colocalized with *NKG7, GNLY* and *CD8A* (NK cells and $CD8^+$ CTL), as well as *TNF* with *CD14*. GSEA using previously-reported gene modules for cytotoxic $CD8^+$ T cells (CTL) in established RA ST confirmed the CTL annotation (**Fig. 1B**, Zhang, et al. [14]). Furthermore, pseudotime trajectory analysis also supported that C1 was more terminally differentiated than C4 (**Fig. 1C**). C6 was the only cytotoxic $CD4^+$ cluster and was enriched in a cytotoxic $CD4^+$ signature as described recently for cytotoxic SARS-CoV-2-reactive $CD4^+$ T Cells in COVID-19 patients (**Fig. 1B**, Meckiff, et al. [15]).
By comparative UMAP analysis, ST was enriched in $CD4^+$ Treg (p=0.023, paired t test) and depleted in naïve-like $CD4^+$ (p=0.0047, paired t test) and $CD8^+$ (p=0.052, paired t test) T cells compared to PB (**Fig. 1D**).

ST expanded clonotypes include $CD8^+$ cytotoxic T cells, and $CD4^+$ T cells with signatures of activation, tissue residency and helper function

Interrogation of single TCR α/β sequences and paired transcriptomic information in the ST dataset identified clonally expanded T cells in all samples except ST1 (**Fig. 2B**; left), despite differences in cellularity (**Fig. 2A**). After UMAP overlay (**Fig. 2B**; right), we observed that expanded ST clonotypes displayed polyfunctional cytotoxic $CD8^+$ Teff (in 3/3 ST), $CD4^+$ memory tissue-resident-like ($CD69^+$), Th2-like ($GATA3^+$) and central memory-like ($ICOS^+$, IL-6 responsive) transcriptomic profiles (in 2/3 ST; **Fig. 2B** and **C**). $CD4^+$ ST clonotypes displayed extensive divergence in phenotype, suggesting plasticity between $CD4^+$ T cell states, as further supported by trajectory analysis (**Fig. 2D**). The ST sample with the most severe synovitis macroscopically (ST4) had the greatest level of T cell oligoclonality (**Fig. 2B**). Collectively these data demonstrate that, although the degree of oligoclonality in the synovium is patient-specific, expanded tissue clonotypes include polyfunctional $CD8^+$ CTL and $CD4^+$ resident-like memory cells expressing genes associated with IL-6 signalling, B cell interaction and helper function.

Some PB and ST clonotypes identify viral-reactive clones, and a shared clonotype identifies a CMV-reactive clone

Given the dominance of the cytotoxic $CD8^+$ T cell response, we compared PB and ST CDR3 amino acid sequences against the VDJdb database of CDR3 sequences that recognize the common viral antigens EBV and CMV (Shugay, et al. [16]). Although none of our TCRα/β sequences matched both a reported anti-viral CDR3α and corresponding CDR3β motif, we found identical matches to individual reported viral-specific CDR3α or CDR3β motifs. CDR3 sequences with an identical match to either a reported CDR3α or CDR3β motif specific for EBV or CMV are shown as a proportion of the total cytotoxic $CD8^+$ T cell population per

sample (**Fig. 3A**, **B**). We identified T cells matching putative viral-specific clones in all samples, with matches to CMV the most frequent (0.4–48% of the cytotoxic $CD8^+$ T cell population), and including putative CMV-specific clones recognising the IE1 epitope (**Fig. 3B**). Predicted EBV-specific clones recognised the BMLF1, BZLF1 and EBNA3A epitopes (**Fig. 3A**). Intriguingly, a shared clonotype detected in both PB and ST of patient 4 matched an HLA-B7 CMV pp65 RPH-restricted clonotype (**Fig. 3C**).

To identify "TCR specificity/convergence groups" likely to recognise common antigens through shared motifs in the CDR3 sequence, we used the GLIPH (grouping of lymphocyte interactions by paratope hotspots) algorithm [17]. GLIPH analysis revealed 124 TCR convergence groups with shared specificity between patients (**Fig. 3D**). The top 3 out of 4 convergence groups (as defined by the number of TCRs comprising the respective group) included TCRs predicted to be viral-specific clonotypes (**Fig. 3D**).

Furthermore, tetramer staining of patient 4 PBMC confirmed the presence of the predicted HLA-B7 RPH shared clone in PB (**Fig. 3E**). Another predicted viral-specific clone identified in the PB of patient 4 was directed to the TPR pp65 epitope, which was confirmed by HLA-B7 TPR tetramer staining (**Fig. 3E**). Patient 4 also carried HLA-A1, and we identified HLA-A1-restricted YSE $CD8^+$ T cells with tetramers, albeit at low frequency, potentially explaining its absence from the scRNAseq data (**Fig. 3E**).

Together these data indicate that viral antigens drive the greatest extent of convergent recombination within the PB and ST TCR repertoire of 4 recent-onset RA patients, indicating that these TCRs were not detected by chance and represent an antigen-driven response.

T cell clonotypes migrating to ST lodge adjacent to blood vessels and dendritic cells

To visualise the distribution of T cells and T cell clonotypes in ST relative to blood vessels, fibroblasts, macrophages and DCs, we stained and imaged ST of patient 4 with imaging mass cytometry. We included TCR Vβ2 and Vβ21.3 mAb as TCR sequencing in ST of this patient identified a *TRBV20-1* $CD8^+$ CTL clonotype and a *TRBV11-2* $CD4^+$ Th2 clonotype. In the lining layer, we identified HLA-DR^+CD68^+ macrophages and $PDPN^+CD90^-$ fibroblasts, punctuated by $Clec9A^+$ DCs (**Fig. 4A**, **B**, **C**, **D**). $CD90^+$ fibroblasts surrounding $CD31^+$ blood vessels (**Fig. 4A**, **B**) were themselves surrounded by HLA-DR^+CD14^+ APCs, likely monocyte-derived DCs (**Fig. 4B**, **C**, **E**). $CD4^+$ and $CD8^+$ T cells were located peri-vascularly, and adjacent to these DCs (**Fig. 4D**, **F**, **G**). Granzyme B and TCR Vβ2 staining identified perivascular $CD8^+$ CTL clonotypes (**Fig. 4F**, **G**, **H**) and TCR Vβ21.3 staining depicted the perivascular $CD4^+$ Th2 clonotype (**Fig. 4G**, **I**). Thus, IMC staining corroborated the phenotype suggested by our combined transcriptomic and TCR analysis. By immunohistochemistry, IL-6 was predominantly expressed in the peri-vascular region, confirming the gene expression, and TNF in the peri-vascular region, and particularly the lining layer (**Fig. 4J**, **K**).

References

1. Orr, C. et al. Synovial tissue research: a state-of-the-art review. *Nat Rev Rheumatol* **13**, 463-475 (2017).
2. Corsiero, E. et al. Single cell cloning and recombinant monoclonal antibodies generation from RA synovial B cells reveal frequent targeting of citrullinated histones of NETs. *Ann Rheum Dis* **75**, 1866-75 (2016).
3. Demoruelle, M.K., Wilson, T.M. & Deane, K.D. Lung inflammation in the pathogenesis of rheumatoid arthritis. *Immunol Rev* **294**, 124-132 (2020).
4. O'Neil, L.J. & Kaplan, M.J. Neutrophils in Rheumatoid Arthritis: Breaking Immune Tolerance and Fueling Disease. *Trends Mol Med* **25**, 215-227 (2019).
5. Serafini, B., Rosicarelli, B., Veroni, C., Mazzola, G.A. & Aloisi, F. Epstein-Barr Virus-Specific CD8 T Cells Selectively Infiltrate the Brain in Multiple Sclerosis and Interact Locally with Virus-Infected Cells: Clue for a Virus-Driven Immunopathological Mechanism. *Journal of Virology* **93**, e00980-19 (2019).
6. Prendergast, C.T. et al. Visualising the interaction of CD4 T cells and DCs in the evolution of inflammatory arthritis. *Annals of the Rheumatic Diseases* **77**, 579-588 (2018).
7. Imberti, L. et al. Reduced T-cell repertoire restrictions in abatacept-treated rheumatoid arthritis patients. *Journal of Translational Medicine* **13**, 12 (2015).
8. Scarsi, M., Ziglioli, T. & Airo, P. Decreased circulating CD28-negative T cells in patients with rheumatoid arthritis treated with abatacept are correlated with clinical response. *J Rheumatol* **37**, 911-6 (2010).
9. Scarsi, M., Ziglioli, T. & Airo, P. Baseline numbers of circulating CD28-negative T cells may predict clinical response to abatacept in patients with rheumatoid arthritis. *J Rheumatol* **38**, 2105-11 (2011).

10. Bergot, A.S. et al. Regulatory T Cells Induced by Single-Peptide Liposome Immunotherapy Suppress Islet-Specific T Cell Responses to Multiple Antigens and Protect from Autoimmune Diabetes. *J Immunol* **204**, 1787-1797 (2020).
11. Ye, L. et al. LncRNA Neat1 positively regulates MAPK signaling and is involved in the pathogenesis of Sjögren's syndrome. *Int Immunopharmacol* **88**, 106992 (2020).
12. Morimoto, Y. et al. Amphiregulin-Producing Pathogenic Memory T Helper 2 Cells Instruct Eosinophils to Secrete Osteopontin and Facilitate Airway Fibrosis. *Immunity* **49**, 134-150.e6 (2018).
13. Qiu, X. et al. Reversed graph embedding resolves complex single-cell trajectories. *Nature Methods* **14**, 979-982 (2017).
14. Zhang, F. et al. Defining inflammatory cell states in rheumatoid arthritis joint synovial tissues by integrating single-cell transcriptomics and mass cytometry. *Nature Immunology* **20**, 928-942 (2019).
15. Meckiff, B.J. et al. Imbalance of Regulatory and Cytotoxic SARS-CoV-2-Reactive CD4(+) T Cells in COVID-19. *Cell* **183**, 1340-1353.e16 (2020).
16. Shugay, M. et al. VDJdb: a curated database of T-cell receptor sequences with known antigen specificity. *Nucleic Acids Res* **46**, D419-d427 (2018).
17. Glanville, J. et al. Identifying specificity groups in the T cell receptor repertoire. *Nature* **547**, 94-98 (2017).

Figures

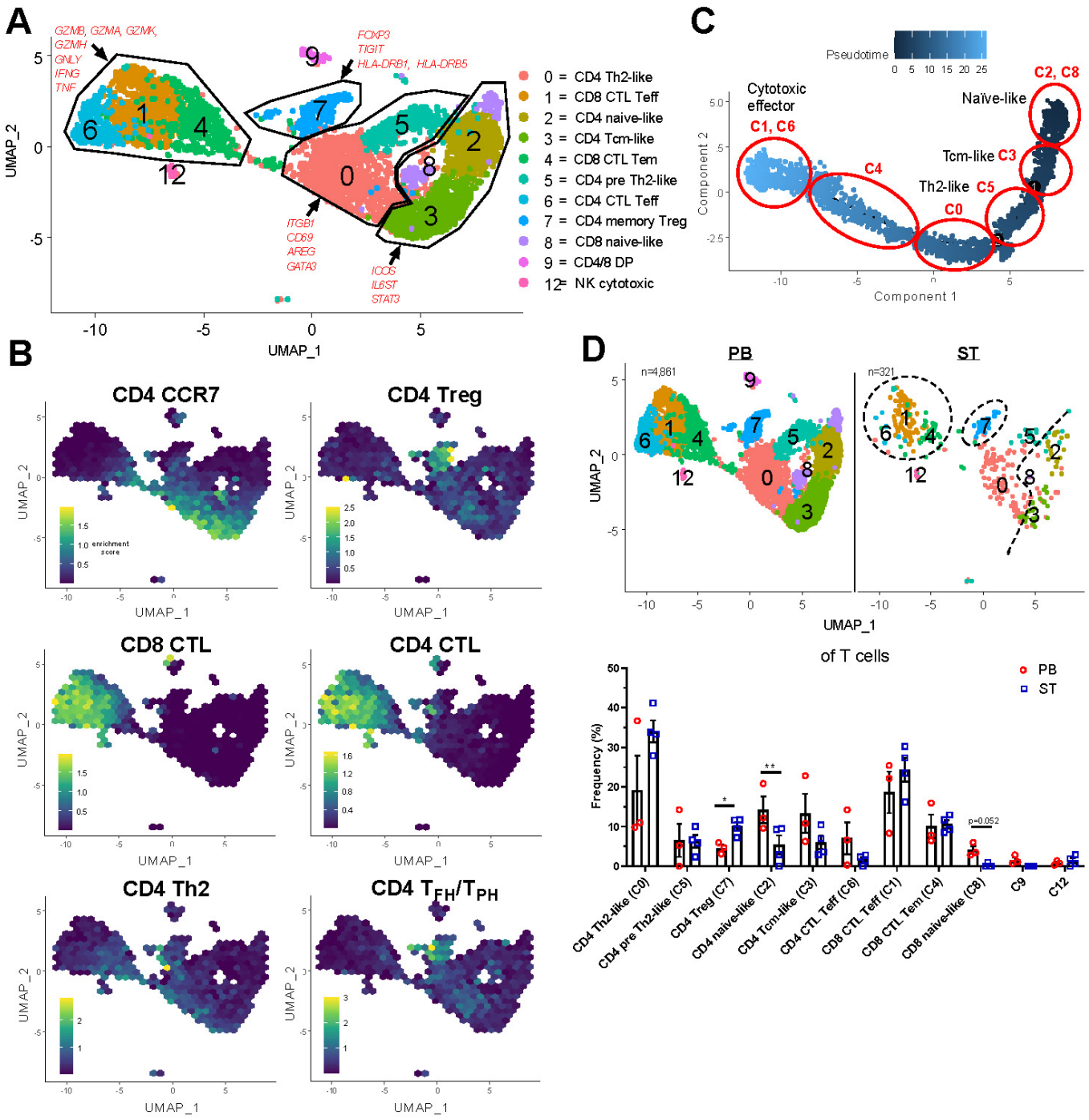

Figure 1. Definition of four T cell superclusters in PB and ST, with enrichment of Th2 and cytotoxic effector T cells in ST. A. Sub-clustering of all CD3$^+$TCR$^+$ cells resulted in the 4 super clusters shown in the UMAP plot of 5,182 cells from combined PB and ST (*n=4* patients; *n=3* for PB; *n=4* for ST). Sub-clusters were manually annotated. **B.** UMAP plots displaying the enrichment scores of CD4 CCR7$^+$, CD4 Treg, CD8 CTL, CD4 CTL, CD4 Th2 and CD4 T_{FH}/T_{PH} signatures. **C.** Pseudotime trajectory analysis using Monocle 2. Cells on the tree are coloured by pseudotime assignment. Manual annotation depicts the approximate position of enrichment of each Seurat cluster on the trajectory. **D.** UMAP plots comparing PB (left) (4,861) and ST (right) (321) CD3$^+$TCR$^+$ cell clusters and quantification of cluster distribution. Paired *t* test, * = $p < 0.05$, ** = $p < 0.01$. Exact *p* value CD4 naïve-like = 0.0047, CD4 Treg = 0.023. Error bars represent SEM.

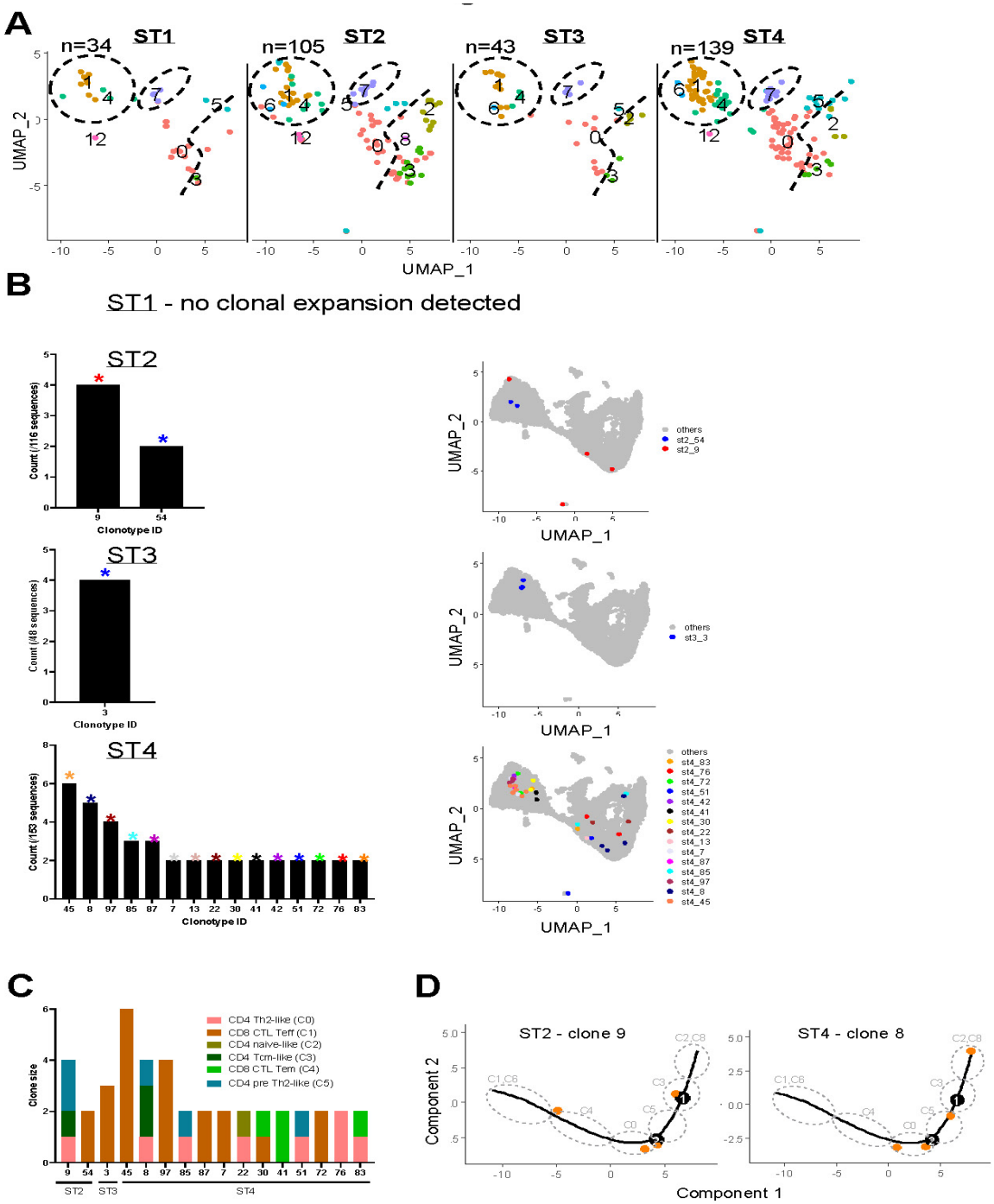

Figure 2. ST expanded clonotypes include CD8⁺ cytotoxic T cells, and CD4⁺ T cells with signatures of activation, tissue residency and helper function. A. Comparative UMAP plots depicting only ST CD3⁺TCR⁺ cells for each of the 4 RA patients. Colour coding and cluster names are as in Figure 2. **B.** Bar plots of clone frequency based on the V(D)J library (left). Only full-length, productive, paired TCRα/β sequences were retained for analysis (Methods) and all clones represented in the bar plots have a CDR3 frequency ≥2 (i.e. clonally expanded). All expanded clones for each patient in the ST are overlayed and coloured onto the UMAP (right) in order to map the transcriptome of the clonotypes. Cells that are not overlayed are depicted as grey in the background to outline the shape of the UMAP space. **C.** Phenotypes of single cells belonging to the same TCR clone (all clones per patient shown in **B** are represented). Each bar is coloured corresponding to the individual phenotypes of single cells within the clone. **D.** Representative trajectories of two expanded clones (coloured in orange) from ST samples. Manual annotation in grey dotted lines depicts the approximate position of enrichment of each Seurat cluster on the trajectory. The 1 and 2 indicate minor branch points.

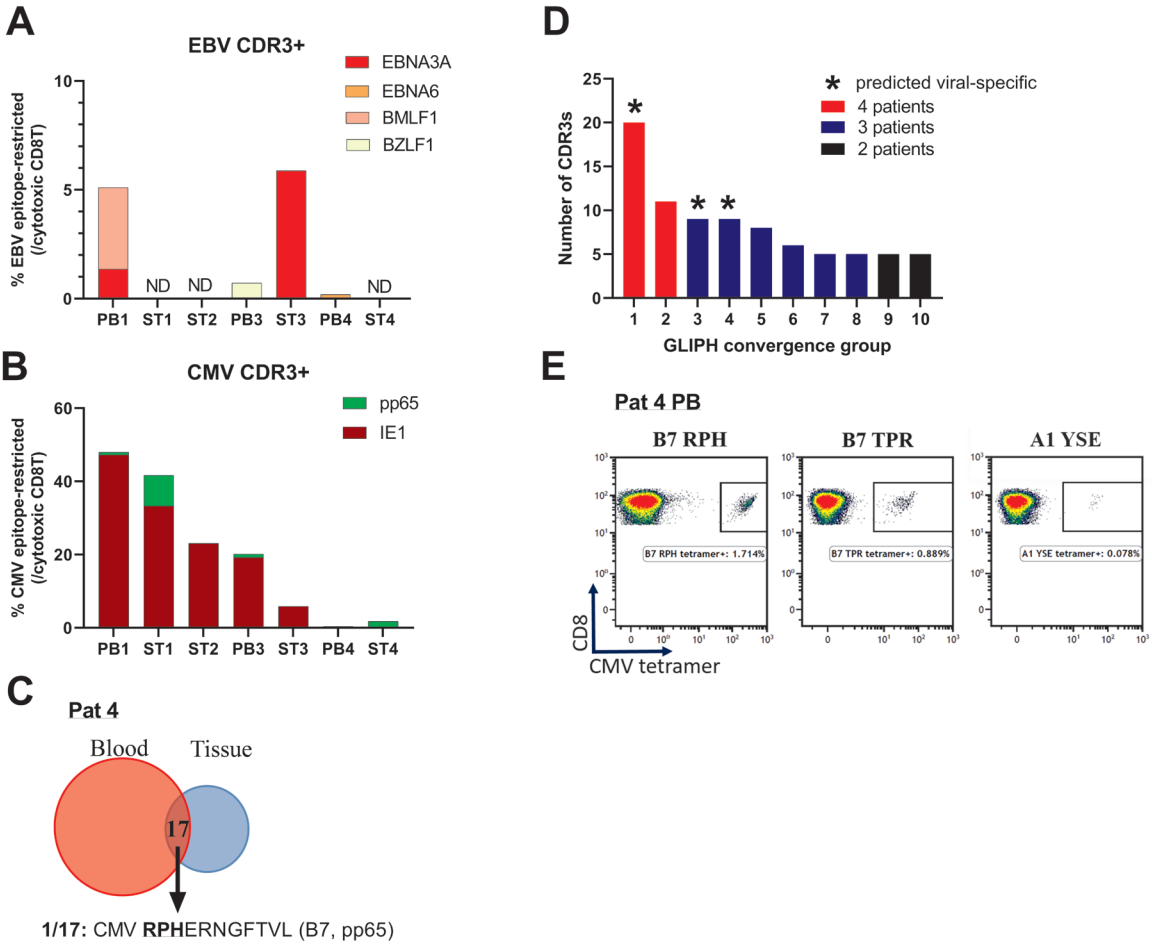

Figure 3. Some PB and ST clonotypes identify viral-reactive clones, and a shared clonotype identifies a CMV-reactive clone. A-B. Bar plots depicting the proportion of the $CD8^+$ CTL compartment contained in putative EBV epitope-restricted (**A**) and CMV epitope-restricted (**B**) clonotypes obtained from the VDJdb database. Colours of the bars represent proportion predicted to be specific for particular viral epitopes. **C.** Shared clonotype from patient 4, which matched a putative CMV pp65 RPH-restricted clone. **D.** Top 10 GLIPH (grouping of lymphocyte interactions by paratope hotspots) convergence groups, coloured by the number of patients comprising each group. The convergence groups containing predicted viral-specific TCRs are depicted with an asterisk. **E.** Tetramer staining of patient 4 PBMC using HLA-B7-pp65 $RPHERNGFTVL_{265\text{-}275}$, HLA-B7-pp65 $TPRVTGGGAM_{417\text{-}426}$ and HLA-A1-pp65 $YSEHPTFTSQY_{363\text{-}373}$ tetramers.

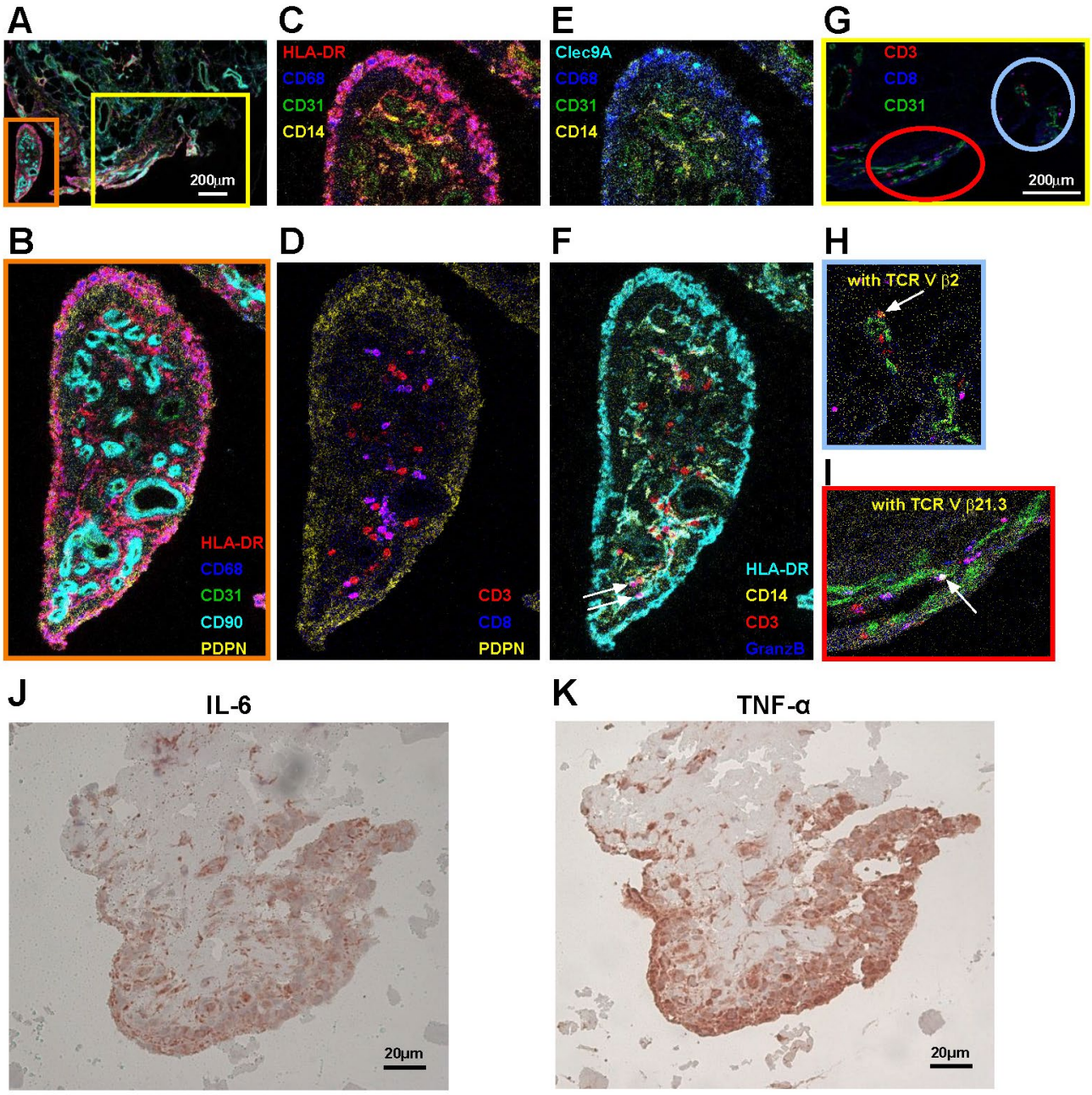

Figure 4. T cell clonotypes migrating to ST lodge adjacent to blood vessels and dendritic cells. A. Prepared slides from patient 4 were ablated on the Hyperion Imaging System, by a UV-laser spot-by-spot at a resolution of 1 µm and a frequency of 200 Hz. The full region of interest selected with 2,100 x 1,000 µm is shown with scalebar in **A**. Representative tissue sections boxed in orange and yellow were selected for detailed further marker investigations in **B**-**F** and **G**-**I** respectively. **B.** HLA-DR^{+}CD68^{+} macrophages (purple) and CD90^{-} podoplanin (PDPN)$^{+}$ fibroblasts (yellow) in the lining layer of the villus with CD90^{+} fibroblasts (light blue) surrounding CD31^{+} blood vessels (green). **C.** HLA-DR^{+}CD14^{+} DCs (orange) surrounding CD31^{+} blood vessels (green). **D.** CD4^{+} (red) and CD8^{+} (purple) T cells in the sub-lining. **E.** Perivascular CD14^{+} DCs (yellow) and lining layer Clec9A^{+} DCs (light blue) and CD68^{+} macrophages (dark blue). **F-I.** Based on the regions of interest circled in **G**, Granzyme B^{+} (purple, **F**) and TCR Vβ2^{+} (orange, **H**) perivascular CD8^{+} CTL clonotype, and TCR Vβ21.3^{+} (white, **I**) perivascular CD4^{+} Th2 clonotype. **J-K.** IHC staining for IL-6 (**J**) and TNF (**K**) on DMARD-naïve synovial tissue section of patient 2 (magnification 40x).